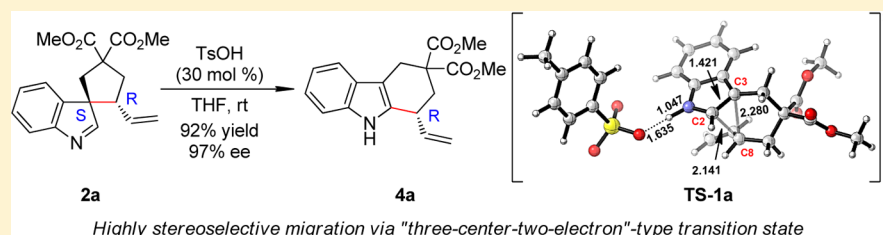


A Combined Theoretical and Experimental Investigation into the Highly Stereoselective Migration of Spiroindolenines

Chao Zheng,* Qing-Feng Wu, and Shu-Li You*

State Key Laboratory of Organometallic Chemistry, Shanghai Institute of Organic Chemistry, Chinese Academy of Sciences, 345 Lingling Lu, Shanghai 200032, China

S Supporting Information

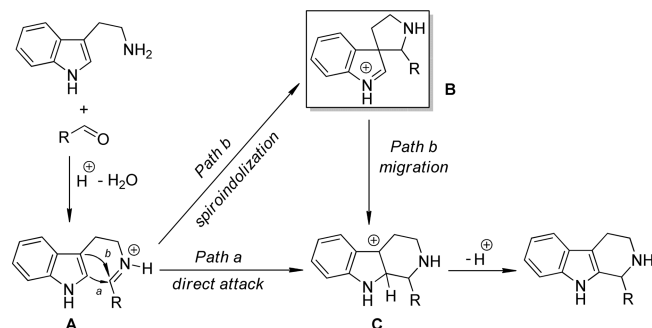


ABSTRACT: This paper describes a combined theoretical and experimental investigation into the acid-catalyzed migration of spiroindolenines to the corresponding fused cyclic products. It is suggested that the "three-center-two-electron"-type transition state is the crucial reason accounting for the highly stereoselective phenomenon. Further studies demonstrated that the electronic property of the migratory group as well as the ring size may have a major influence on the reaction profile of the migration process. Some predictions based on the computational results were supported by additional experiments.

INTRODUCTION

The Pictet–Spengler reaction¹ is among the most powerful methods for functionalization at the C2 position of indoles. It also provides quick access to various polycyclic indole derivatives including tetrahydro- β -carbolines² that are widely distributed in natural products as well as molecules of pharmaceutical interests. However, the detailed mechanism of the Pictet–Spengler reaction and related functionalization at the C2 position of indoles still remains a debate.^{1f} In general, two mechanistic scenarios have been proposed (Scheme 1): the product of Pictet–Spengler-type reaction can be obtained either via the direct attack of the C2 position of indole to the iminium moiety (path a) or, alternatively, through the nucleophilic addition of the C3 position of indole, affording

Scheme 1. Two Different Mechanisms Commonly Proposed for Pictet–Spengler and Related Reactions



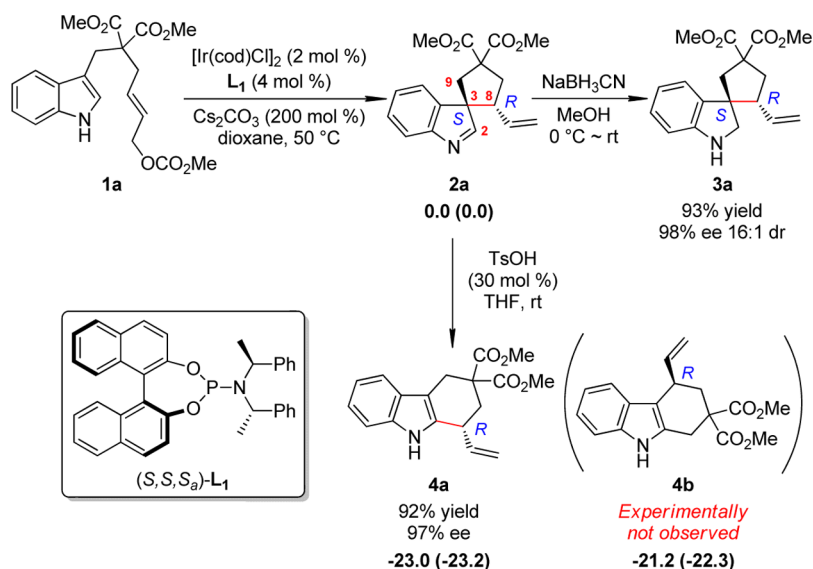
the spiroindolenine species that could undergo subsequent migration process (path b).

A large amount of experimental evidence supporting path b has been reported. It is known that the five-membered azaspiroindolines can be generated by the condensation of tryptamine and the corresponding aldehyde under reductive conditions.³ The pioneering works of Jackson et al.⁴ showed that the independently synthesized 3,3-disubstituted spiroindolenines undergo an intramolecular rearrangement affording the 2,3-disubstituted indole counterparts in acidic media.⁵ Computational methods have also been employed to probe the mechanism of Pictet–Spengler reaction, but the results seemed not to support the spiroindolization/migration mechanism.⁶ In a recent mechanistic study, Stöckigt, Peters, O'Connor, and co-workers⁷ calculated a nonenzyme-catalyzed Pictet–Spengler reaction with the DFT method (PW1PW91) and showed that the protonated spiroindolenine (**B**, R = Me) is a nonproductive intermediate. The migration process (**B** \rightarrow **C**, R = Me) does not occur, and the spiroindolenine only rearranges to reform the iminium species (**A**, R = Me). Indeed, the nature of the migration of the spiroindolenines still remains unclear and requires further exploration. Meanwhile, the direct stereochemistry information associated is also not fully uncovered, probably due to the difficulty in synthesizing enantioenriched spiroindolenines.

Recently, we⁸ disclosed that chiral five-membered spiroindolenine **3a** could be synthesized by Ir-catalyzed intramolecular asymmetric allylic dearomatization⁹ of indol-3-yl allylic

Received: February 19, 2013

Published: April 11, 2013

Scheme 2. Ir-Catalyzed Intramolecular Asymmetric Allylic Dearomatization of Indol-3-yl Allylic Carbonate and Acid-Catalyzed Highly Stereoselective Allyl Migration of Spiroindolenine^a

^a ΔG_{THF} and ΔE_{THF} (in parentheses) of compounds 2a, 4a, and 4b are in kcal/mol. Calculated at the PBE1PBE/6-311+G(d,p) level of theory.

carbonate 1a and subsequent NaBH₃CN reduction of the spiroindolenine compound 2a (Scheme 2). The products were obtained in excellent yields and stereoselectivities (up to 96% yield, 99% ee and 16:1 dr) under mild conditions. More intriguingly, on treatment of catalytic amount of TsOH, the spiroindolenine 2a was converted to the corresponding tetrahydrocarbazole 4a smoothly, with the ee's of the products as well as the absolute configuration of the chiral center at the allylic position conserved. To the best of our knowledge, this is the first observation of highly stereoselective migration of optically active chiral spiroindolenines. In addition, it also provides a unique opportunity for the mechanistic research of intramolecular C2 alkylation of indoles, especially for the details of the migration process. Herein, we present our theoretical investigation into this highly stereoselective migration of spiroindolenines which suggests that the “three-center-two-electron”-type transition state is crucial for the maintenance of chirality at the allylic position. Further studies on other related models showed that the electronic property of the migratory group and the ring size of the spiroindolenines have pronounced effects on the reaction pathway as well as the stereochemistry of the migration process. Some predictions based on the computational results were supported by additional experiments.

RESULTS AND DISCUSSION

Reaction Mechanisms. We started our study by comparing the thermodynamic stabilities of spiroindolenine and tetrahydrocarbazole products (Scheme 2). There are two chiral centers in the spiroindolenine 2a; thus, two pairs of diastereomers exist. In this paper, we only present the reaction profile of the (3*S*,8*R*) isomer according to the experimental results. As expected, both the allyl migration product 4a (-23.0 kcal/mol) and the product of methylene migration 4b (-21.2 kcal/mol), which is not observed experimentally, are significantly more stabilized than 2a (0.0 kcal/mol), probably due to the recovery of the aromaticity of the indole ring in the

tetrahydrocarbazole products. These results verified the migration process is highly favored thermodynamically.

The migration reaction was conducted in the presence of a catalytic amount of acid. Therefore, the complex of the indol-3-yl allylic carbonate and tosylate acid (5a) was set as the reference for the migration process (Figure 1). The transition state for the allyl migration (TS-1a) was located with an energetic barrier of 19.5 kcal/mol. The intrinsic reaction coordinate (IRC) calculation indicated that the migration process is concerted (see the Supporting Information for details). TS-1a connects directly to 5a and the corresponding tosylate-bound protonated tetrahydrocarbazole 6a (4.6 kcal/mol). Both the bond formation of C2–C8 and the bond cleavage of C3–C8 are involved in one single step ($B(\text{C}2\cdots\text{C}8) = 2.141 \text{ \AA}$, $B(\text{C}3\cdots\text{C}8) = 2.280 \text{ \AA}$ in TS-1a). The geometric feature of TS-1a reveals a “three-center-two-electron”-type structure. The HOMO of TS-1a ($E = -6.7 \text{ eV}$) clearly showed the electronic interaction between the indole ring and the migratory allyl group. One *p* orbital of C8 bridges over the π orbital of the C2–C3 bond (Figure 2), which is similar to the structure of the corner-protonated cyclopropane or nonclassical carbocations¹⁰ that are often involved in the pinacol and Wagner–Meerwein rearrangement.¹¹ We believe the “three-center-two-electron”-type transition state is the critical reason that accounts for the highly stereoselective phenomenon. The allyl group keeps interacting with the C2–C3 bond of the indole ring, and no “free” allyl carbocation is formed during the migration process. Therefore, the chirality of C8 can be reserved and no racemization happens. Subsequently, the proton at the C2 position of intermediate 6a is readily abstracted by the tosylate anion (TS-2a, 7.7 kcal/mol) to afford the complex of the chiral tetrahydrocarbazole and tosylate acid (7a, -9.2 kcal/mol). In addition, all efforts aimed at locating an intermediate possessing a free allyl carbocation (8a'), which is an analogue of 8d' and 8e' (vide infra), failed. Instead, we obtained a multisubstituted 2*H*-furanium intermediate 8a (22.6 kcal/mol) that is formed via nucleophilic attack of one carbonyl oxygen atom of the ester group to the allyl moiety. The energy of the transition state leading to this intermediate (TS-5a, 35.0

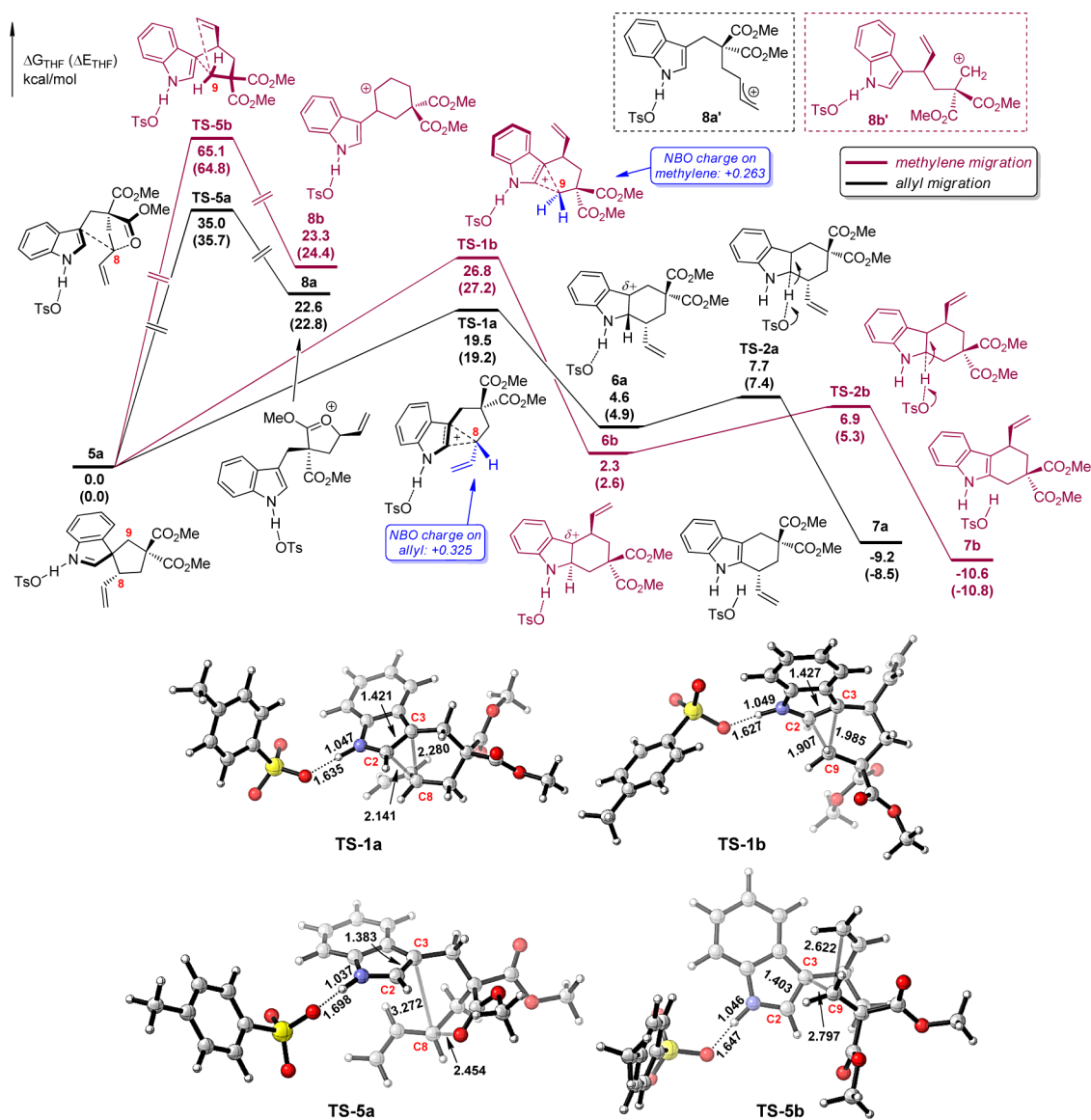


Figure 1. Reaction profile of TsOH-catalyzed allyl/methylene migration of spiroindolenine 2a and the optimized structures of TS-1a, TS-1b, TS-5a, and TS-5b. Calculated at PBE1PBE/6-311+G(d,p) level of theory. $\Delta G_{\text{THF}}^{\ddagger}$ and $\Delta E_{\text{THF}}^{\ddagger}$ (in parentheses) are in kcal/mol. Bond distances are in angstroms.

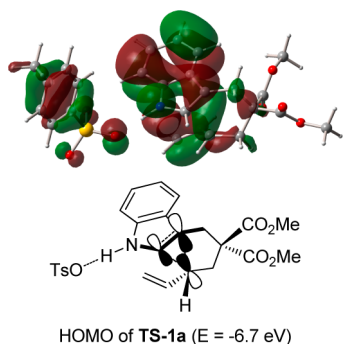


Figure 2. Calculated HOMO of TS-1a.

kcal/mol) is quite high. These results further support that the allyl migration is concerted and no free allyl carbocation is likely to be involved in this process.¹²

Although the alkyl migration of 3,3-disubstituted indolenines is known in the literature,¹³ the methylene migration of C9 was

not observed in the current system. We studied the methylene migration of complex 5a (Figure 1), and TS-1b (26.8 kcal/mol) was found for this methylene migration. The energetic barrier of TS-1b is substantially higher than that of TS-1a by 7.3 kcal/mol, which is in accord with the experimental observations. Although TS-1b also features a “three-center-two-electron”-type structure, the distances between the migratory carbon (C9) and indole C2–C3 bond ($B(\text{C}2\cdots\text{C}9) = 1.907$ Å, $B(\text{C}3\cdots\text{C}9) = 1.985$ Å) are somewhat shorter compared to the corresponding values in TS-1a. We reasoned that the energetic difference and the structural deviation between TS-1a and TS-1b are the reflection of different abilities of allyl and methylene in stabilizing the positive charge. NBO charge analyses indicated the sum of positive charge that distributes over the allyl moiety in TS-1a is +0.325 while the positive charge possessed by the migratory methylene group in TS-1b is only +0.263.¹⁴ Since the methylene group is a poorer electron-donating group than the allyl group, a stronger interaction between it and indole ring should be required to

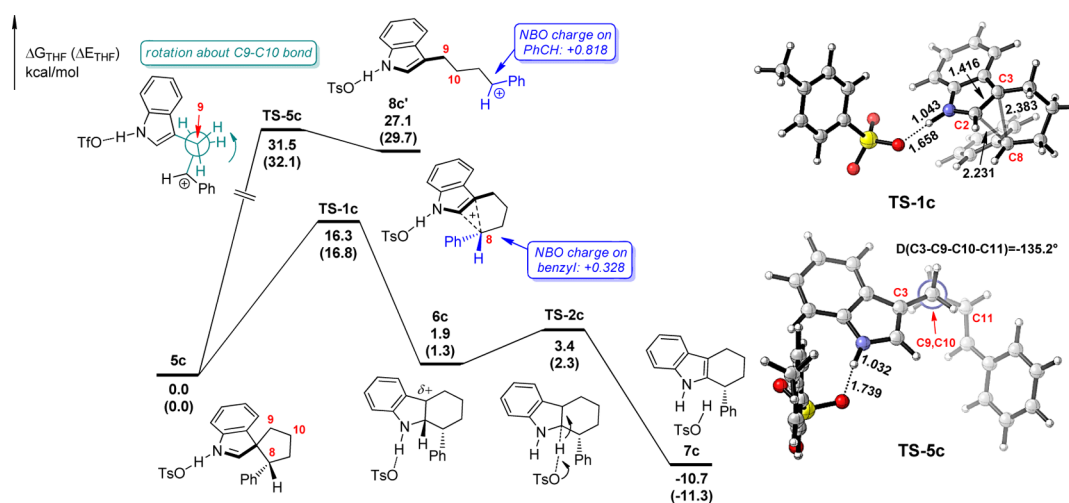


Figure 3. Reaction profile of TsOH-catalyzed benzyl migration and the optimized structures of TS-1c and TS-5c. Calculated at PBE1PBE/6-311+G(d,p) level of theory. ΔG_{TSF} and ΔE_{TSF} (in parentheses) are in kcal/mol. Bond distances are in angstroms.

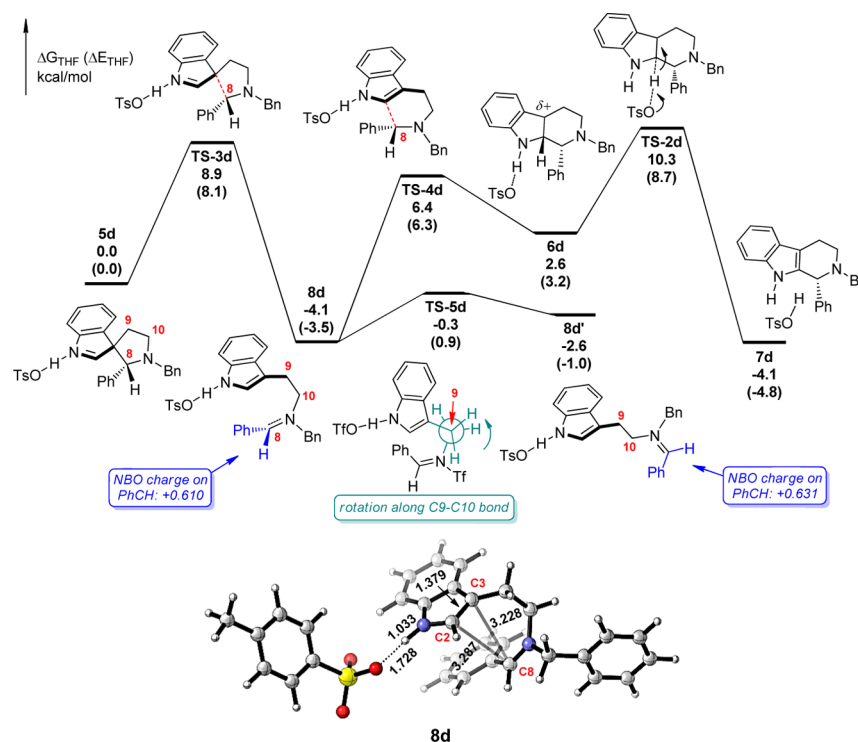


Figure 4. Reaction profile of TsOH-catalyzed rearrangement of N-Bn aza-spiroindolenine and the optimized structure of intermediate 8d. Calculated at PBE1PBE/6-311+G(d,p) level of theory. ΔG_{TSF} and ΔE_{TSF} (in parentheses) are in kcal/mol. Bond distances are in angstroms.

stabilize the positive charge during the migration process. The electron-rich indole ring interacts with the methylene group more significantly than with the allyl group, which makes the NBO charge on methylene in TS-1b less positive. Meanwhile, the strong interaction brings the migratory methylene and indole moiety closer in TS-1b and raises its energy as well. Like the case of allyl migration mentioned above, the intermediate with a free terminal methylene carbocation (**8b'**) does not exist. Instead, this methylene carbocation can be stabilized by the allyl moiety to form a cyclohexanylium intermediate (**8b**, 23.3 kcal/mol). However, the transition state that connects **8b** and the starting complex (TS-5b, 65.1 kcal/mol) is energetically inaccessible.

Influence of the Electronic Property of the Migratory Group. The above results implicate the importance of the electronic property of the migratory group on the transition state of migration process. Thus, we decided to test the migration processes with other migratory groups computationally. As depicted in Figure 3, the TsOH-catalyzed rearrangement of phenyl-substituted spiroindolenine was considered.¹⁵ The relative energy and the structural characters of the transition state for the benzyl migration (TS-1c, 16.3 kcal/mol) are rather similar to those of the allyl migration. The benzyl migration is still concerted with the migratory carbon (C8) keeping interaction with the indole moiety in TS-1c (B(C2...C8) = 2.231 Å, B(C3...C8) = 2.383 Å). The NBO charge on the benzyl group (+0.328) is only slightly more

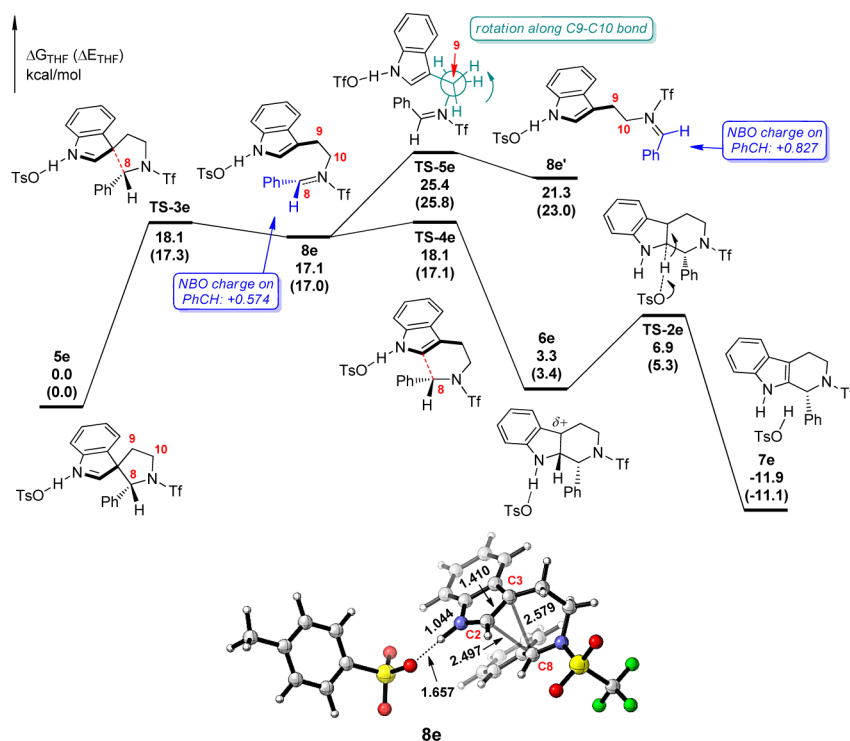


Figure 5. Reaction profile of TsOH-catalyzed rearrangement of N-Tf aza-spiroindolenine and the optimized structure of intermediate **8e**. Calculated at PBE1PBE/6-311+G(d,p) level of theory. $\Delta G_{\text{THF}}^{\ddagger}$ and $\Delta E_{\text{THF}}^{\ddagger}$ (in parentheses) are in kcal/mol. Bond distances are in angstroms.

positive than the allyl group in **TS-1a**. On the other hand, the intermediate with a free benzyl carbocation (**8c'**, 27.1 kcal/mol), an analogue of **8d'** and **8e'** (vide infra), is rather unstable, and its formation is also kinetically unfavorable (**TS-5c**, 31.5 kcal/mol). These calculations suggest the benzyl migration in achiral acidic media may also be a highly stereoselective process if enantioenriched phenyl-substituted spiroindolenine could be prepared.

What if the migratory group has a much stronger ability to stabilize the positive charge than allyl and benzyl groups? We regarded the aza-spiroindolenines with aryl iminium as the latent migratory group to be proper models. The rearrangement of this type of substrates may be closely related to the mechanism of the Pictet–Spengler reaction. Since the protecting group on the nitrogen could also affect the electronic property of the imine group significantly, we considered two additional model systems with either a benzyl (**5d**) or a triflate (**5e**) group attached on the imine nitrogen atom.¹⁶ Different from the concerted migrations of the allyl, methylene, and benzyl groups mentioned above, the rearrangements of these two aza-spiroindolenines to their corresponding tetrahydro- β -carboline are stepwise. The bond cleavage of C3–C8 of **5d** is quite facile (**TS-3d**), and its energetic barrier is only 8.9 kcal/mol (Figure 4). The N-Bn iminium intermediate **8d** generated is rather stable (–4.1 kcal/mol). Subsequently, the iminium carbon (C8) is easily attacked by the C2 position of indole ring (**TS-4d**, 6.4 kcal/mol), affording the protonated N-Bn tetrahydro- β -carboline intermediate (**6d**, 2.6 kcal/mol). The final TsOH-bound product **7d** (–4.1 kcal/mol) is obtained after the deprotonation step (**TS-2d**, 10.3 kcal/mol). However, the optimized structure of the key intermediate **8d** reveals that the N-Bn aryl iminium motif has little interaction with the indole ring. The distances of C2...C8 and C3...C8 in **8d** are 3.287 and 3.228 Å, respectively. The energetic barrier of

rotation about C9–C10 bond (**TS-5d**) is only 3.8 kcal/mol, making the linear form of the N-Bn aryl iminium intermediate **8d'** (–2.6 kcal/mol) readily accessible. The NBO charges distributed over the PhCH segments of **8d** (+0.610) and **8d'** (+0.631) are similar in value, which may imply that no remarkable charge transfer exists between the indole ring and the N-Bn aryl iminium moiety in **8d** and the positive charge can be stabilized well by the N-Bn group itself due to its electron-donating nature.¹⁷ These results suggest the fast racemization at the C8 position must happen during this rearrangement process and no enantioenriched product can be obtained if the enantioenriched N-Bn aza-spiroindolenine is exposed in an achiral acidic environment.¹⁸

On the contrary, the reaction profile of the TsOH-catalyzed rearrangement of N-Tf aza-spiroindolenine is noteworthy (Figure 5). The energetic barrier of C3–C8 bond cleavage (**TS-3e**) is 18.1 kcal/mol, which is much higher than its N-Bn counterpart and comparable to that of the allyl and benzyl migration. The N-Tf iminium intermediate **8e** (17.1 kcal/mol) is then attacked by the C2 position of indole (**TS-4e**, 18.1 kcal/mol) to generate the protonated N-Tf tetrahydro- β -carboline (**6e**, 3.3 kcal/mol). The potential energy surface is quite flat from **TS-3e** to **TS-4e**, and only minor structural shifts can be observed for these two transition states and the key intermediate **8e**. More importantly, the distances of C2...C8 and C3...C8 in **8e** are 2.497 and 2.579 Å, respectively, much shorter than that observed in the N-Bn analogue **8d** and only slightly longer than the distances of C2...C8 and C3...C8 in **TS-1a** for allyl migration. This structural character implicates that there must be some interaction between the N-Tf aryl iminium motif and indole ring in **8e**. Indeed, the second-order perturbation theory analysis on the basis of NBOs suggests a significant donor–acceptor interaction between these two moieties. The stabilization energy $E(2)$ from the “filled”

$\pi(C2-C3)$ orbital to the “empty” $p^*(C8)$ orbital is estimated to be 74.38 kcal/mol for **8e**.¹⁹ As a result, the rotation about C9–C10 bond (TS-**5e**, 25.4 kcal/mol) breaking such interaction is energetically highly unfavorable. The linear form of the N-Tf aryl iminium **8e'** (21.3 kcal/mol) is also unstable relative to **8e**. Analysis of the NBO charges that are distributed over the PhCH segments of **8e** (+0.574) and **8e'** (+0.827) led to a similar conclusion. The much less positive charge possessed by the PhCH segment of **8e** could be explained by some charge transfer from the electron-rich indole ring to the electron-deficient N-Tf aryl iminium moiety. However, this type of stabilization effect cannot exist in **8e'**, and the charge-separate nature raises its energy as well.²⁰ Since the formation of “free” N-Tf aryl iminium species from **8e** is much higher in energy compared with the nucleophilic attack of the C2 position of the indole ring, it suggests that the rearrangement of N-Tf aza-spiroindolenine, although stepwise, might also be a highly stereoselective process.

The influence of the electronic properties of the migratory groups on the reaction profiles of the rearrangements of five-membered spiroindolenines is described in Figure 6. In general,

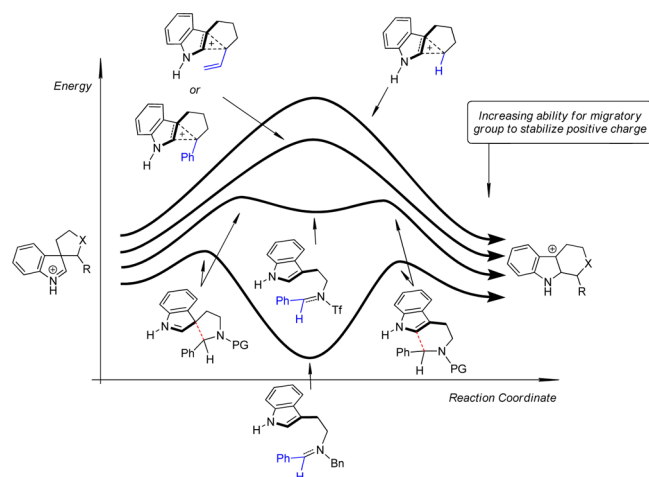
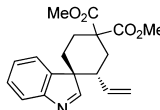
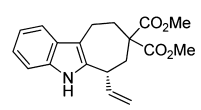
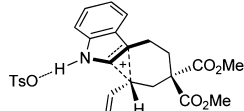
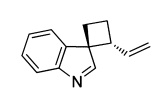
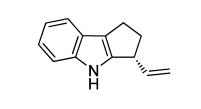
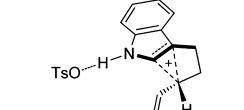
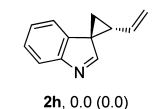
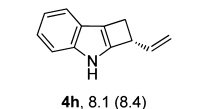


Figure 6. Schematic description for the rearrangements of five-membered spiroindolenines with various migratory groups.

as the ability for the migratory group to stabilize positive charge increases from methylene to N-Bn aryl iminium, the transformation from the spiroindolenines to their corresponding tetrahydrocarbazole or tetrahydro- β -carboline derivatives becomes easier and the reaction shifts from concerted to stepwise. Besides, the rearrangements of methylene, allyl, benzyl, and N-Tf aryl iminium moieties might be highly stereoselective processes because of the “three-center-two-electron”-type transition states or a related key intermediate with close interaction between the migratory group and the indole ring.

Influence of the Ring Size. Next, we explored the influence of the ring size to the reaction profile of the allyl migration. In order to keep consistency with the previous calculations, we only present the results on the allyl migration of the (3*S*,8*R*)-isomers of the six-, four-, and three-membered spiroindolenines **2f–h** (Table 1). Thermodynamically, the seven- and five-membered ring-expansion products **4f** and **4g** are more stabilized than the corresponding starting materials by 18.3 and 29.1 kcal/mol, respectively, whereas the rearrangement of the three-membered-ring analog **2h** is not favored. The Gibbs free energy of **4h** is 8.1 kcal/mol higher than that of **2h**,

Table 1. Calculated Energy of the Spiroindolenines, the Migration Products, and the Corresponding Transition States with Different Ring Sizes^a

 2f , 0.0 (0.0)	 4f , -18.3 (-18.8)	 TS-1f , 24.0 (24.2) ^b
 2g , 0.0 (0.0)	 4g , -29.1 (-29.2)	 TS-1g , 11.7 (11.1) ^b
 2h , 0.0 (0.0)	 4h , 8.1 (8.4)	<i>TS for migration not found</i>

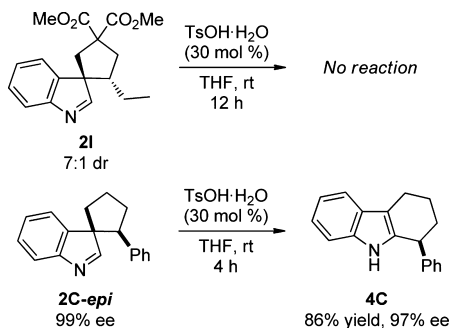
^aCalculated at PBE1PBE/6-311+G(d,p) level of theory. ΔG_{THF} and ΔE_{THF} (in parentheses) are in kcal/mol. ^bEnergetic barrier relative to the complexes of the corresponding spiroindolenines and tosylate acid.

indicating the energy cost due to the fact that formation of the strained cyclobutene motif cannot be compensated with the recovery of aromaticity of the indole ring.

The possibility of the TsOH-catalyzed allyl migration of these three spiroindolenines was also investigated. The allyl [1,2]-shift of **2f** and **2g** can occur through related “three-center-two-electron”-type transition states **TS-1f** and **TS-1g**. Therefore, the retention of configuration at the allylic position is expected. The energetic barrier of **TS-1f** (24.0 kcal/mol) is 4.5 kcal/mol higher than that of **TS-1a**, which suggests the allyl migration affording a seven-membered-ring product requires much harsher reaction conditions. The energetic barrier of **TS-1g** (11.7 kcal/mol), on the other hand, is quite low, an apparent outcome for the formation of energetically favored five-membered ring. It also implies the spiroindolenine **2g** cannot be easily separated and has a strong tendency to migrate.²¹ After several attempts, we could not locate the transition state of acid-catalyzed allyl migration that connects **2h** and **4h**. Further relaxed scan of the potential energy surface (PES) reveals that the energy is increasing monotonously along the conversion from the TsOH-bound **2h** to the “TsOH-bound **4h**” and the latter one is not a stationary point on PES (see the Supporting Information for details). Thus, we might conclude the three-membered spiroindolenine may be stable to some extent and the direct conversion to the cyclobut[b]indole ring system is not likely to operate under mild conditions.

Experimental Validation. Further experimental investigation was carried out to verify the prediction based on the above calculations (Scheme 3). The ethyl-substituted spiroindolenine **2I** (7:1 dr) was synthesized and subjected to the standard conditions of the migration reaction (in this section, we use capital letters to denote the corresponding compounds synthesized experimentally). Not surprisingly, no migration product was observed even with elongated reaction time. This result indicates that the alkyl migration is less effective compared with the allyl migration. In addition, the phenyl-substituted five-membered spiroindolenine **2C-epi** was synthesized. Its relative configuration was established as (3*S**,8*S**) by NOE analysis. In the presence of 30 mol % of TsOH, the

Scheme 3. Experimental Validation



enantiopure **2C-epi** was converted smoothly to the corresponding phenyl-substituted tetrahydrocarbazole **4C** in 4 h in 86% yield and 97% ee. This result demonstrated that no racemization at the benzylic position occurs during the benzyl migration process, which is in well accord with the above calculations.

SUMMARY

In this work, we performed computational studies on the reaction mechanism of the experimentally observed acid-catalyzed highly stereoselective migration of spiroindolenines. The calculated results suggest that the allyl migration of the five-membered spiroindolenine is a concerted reaction through a “three-center-two-electron”-type transition state. This feature also accounts for the highly stereoselective phenomenon because no free carbocation can be formed during the migration process and thus no racemization can occur at the allylic position. The electronic property of the migratory group has pronounced effect on the reaction profile. In general, the acid-catalyzed rearrangement of the spiroindolenine species becomes easier as the ability for migratory group to stabilize positive charge increases. Our calculations suggest that the methylene, benzyl, and even N-Tf aryl iminium migration might be stereoselective processes if the enantioenriched precursors could be synthesized. In addition, the influence of the ring size ($n = 3-6$) to the allyl migration has also been investigated, revealing the migration aptitude as $4 > 5 > 6 > 3$. In addition, some predictions based on the computations have been supported by additional experiments. We believe this detailed mechanistic study will be helpful for deep understanding of the mechanism of the indole C2 functionalization reactions.²² Further exploration to expand the reaction scope based on the present investigation is currently underway in this laboratory.

EXPERIMENTAL SECTION

Computational Methods. All calculations in this paper were performed with the Gaussian09 package.²³ The density functional theory (DFT) method was employed using the PBE1PBE functional.²⁴ The standard 6-311+G(d,p) basis sets were applied for all atoms. Optimizations were conducted without any constraint using SMD model²⁵ in THF ($\epsilon = 7.4257$). Frequency analyses were carried out to confirm each structure being a minimum (no imaginary frequency) or a transition state (only one imaginary frequency). Single-point calculations of some key structures using the M06-2X functional²⁶ were also performed, the results of which are consistent with that obtained using PBE1PBE functional.²⁷ The natural bond orbital (NBO) analyses were performed using NBO 3.1 implemented in Gaussian09. Throughout this paper, we mainly discuss the Gibbs free energies in THF (ΔE_{THF}), unless specified. The electronic energies in

THF including zero-point energy corrections (ΔE_{THF}) are also given in parentheses for reference. All figures of the calculated 3D structures were prepared using CYLview.²⁸

Procedure for Converting Spiroindolenine into Tetrahydrocarbazole. *Synthesis of 2I.* A flame-dried Schlenk tube was cooled to room temperature and filled with argon. To this flask were added [Ir(cod)Cl]₂ (5.4 mg, 0.008 mmol, 2 mol %), phosphoramidite ligand (*S,S,S*_a)-L₁ (8.4 mg, 0.016 mmol, 4 mol %), THF (1.0 mL), and *n*-propylamine (1.0 mL). The reaction mixture was heated at 50 °C for 30 min, and then the volatile solvents were removed in vacuo to give a pale yellow solid. After that, allylic carbonate **1a** (155.6 mg, 0.4 mmol), cesium carbonate (260.3 mg, 0.8 mmol, 200 mol %), and THF (4.0 mL) were added. The reaction mixture was refluxed for 2 h. After the reaction was complete (monitored by TLC), the crude reaction mixture was filtrated with Celite and washed with EtOAc. The solvents were removed under reduced pressure. The product **2a** was used for the next step without further purification.

To a solution of **2a** in anhydrous MeOH (4 mL) was added Pd/C (40.0 mg, 0.04 mol, 0.1 equiv). The reaction mixture was stirred under H₂ atmosphere (1 atm) at rt for 4 h. After the reaction was complete (monitored by TLC), the crude reaction mixture was filtrated with Celite and washed with EtOAc. The solvents were removed under reduced pressure. Then the residue was purified by silica gel column chromatography (PE/EA = 2/1) to afford the desired product **2I**.

2I: white solid (81.9 mg, 65% yield for two steps); ¹H NMR (400 MHz, CDCl₃) δ 0.65 (t, $J = 7.6$ Hz, 3H), 0.70–0.78 (m, 1H), 0.83–0.90 (m, 1H), 2.37 (d, $J = 14.8$ Hz, 1H), 2.48–2.52 (m, 2H), 2.72 (d, $J = 7.2$ Hz, 1H), 3.11 (d, $J = 15.2$ Hz, 1H), 3.77 (s, 3H), 3.83 (s, 3H), 7.23 (dd, $J = 7.6, 6.4$ Hz, 1H), 7.32 (s, 1H), 7.34 (s, 1H), 7.60 (d, $J = 7.6$ Hz, 1H), 8.01 (s, 1H); ¹³C NMR (100 MHz, CDCl₃) δ 12.4, 22.5, 39.0, 40.4, 45.9, 52.9, 53.1, 59.0, 66.2, 121.1, 123.1, 125.9, 127.8, 140.9, 155.3, 171.9, 172.7, 177.6; IR (thin film) ν_{max} (cm⁻¹) = 2957, 1729, 1558, 1437, 1251, 1197, 1173, 1127, 1098, 940, 858, 753; MS (EI-quadrupole, m/z , rel intensity) 247 ([M]⁺, 95), 218 (100); HRMS (ESI-TOF) calcd for C₁₈H₂₂NO₄ [M + H]⁺ 316.1549, found 316.1537; mp = 72.3–73.0 °C.

Migration of 2I. To a solution of spiroindolenine **2I** (63.1 mg, 0.2 mmol, 1.0 equiv) in anhydrous THF (4 mL) was added *p*-toluenesulfonic acid (11.4 mg, 0.06 mmol, 0.3 equiv). The reaction mixture was stirred at rt and monitored by TLC and ¹H NMR. The starting material was recovered after 12 h.

Migration of 2C-epi. To a solution of spiroindolenine **2C-epi** (49.4 mg, 0.2 mmol, 1.0 equiv) in anhydrous THF (4 mL) was added *p*-toluenesulfonic acid (11.4 mg, 0.06 mmol, 0.3 equiv). The reaction mixture was stirred at rt for 4 h. After the reaction was complete (monitored by TLC), the reaction mixture was quenched with saturated aqueous NaHCO₃ and then diluted with water and EtOAc. The organic layer was separated, washed sequentially with water and brine, and dried over Na₂SO₄. The solvents were removed under reduced pressure. Then the residue was purified by silica gel column chromatography (PE/EA = 10/1) to afford the desired product **4C** as a pale yellow oil.

4C: viscous yellow oil (42.4 mg, 86% yield), 97% ee [Daicel Chiralcel OD-H, hexane/2-propanol = 40/1, $\nu = 0.4$ mL·min⁻¹, $\lambda = 254$ nm, $t(\text{minor}) = 30.30$ min, $t(\text{major}) = 31.56$ min]; $[\alpha]_{\text{D}}^{20} = +6.0$ ($c = 0.2$, CHCl₃); ¹H NMR (400 MHz, CDCl₃) δ 1.78–1.92 (m, 2H), 1.99–2.07 (m, 1H), 2.25–2.31 (m, 1H), 2.81–2.84 (m, 2H), 4.13 (dd, $J = 8.0, 5.6$ Hz, 1H), 7.06–7.12 (m, 2H), 7.14–7.17 (m, 3H), 7.22–7.32 (m, 3H), 7.40 (brs, 1H), 7.52 (dd, $J = 6.0, 2.4$ Hz, 1H); ¹³C NMR (100 MHz, CDCl₃) δ 21.0, 22.0, 34.1, 41.5, 110.6, 111.7, 118.1, 119.1, 121.3, 126.7, 127.5, 128.3, 128.6, 135.5, 135.8, 144.2; IR (thin film) ν_{max} (cm⁻¹) = 3057, 2970, 1679, 1619, 1490, 1321, 1081, 1044, 936, 878, 742, 699; MS (EI-quadrupole, m/z , rel intensity) 247 ([M]⁺, 95), 218 (100); HRMS (EI-TOF) calcd for C₁₈H₁₇N [M]⁺ 247.1361, found 247.1363.

The synthetic procedure and characterization of **2C-epi** are given in the Supporting Information.

■ ASSOCIATED CONTENT

■ Supporting Information

Complete citation of ref 23, calculation details including the figures and tables not presented in the text, 3D structures and Cartesian coordinates for all calculated stationary points, synthetic procedure and characterization of **2C-epi**, and copies of the ^1H , ^{13}C NMR and HPLC spectra. This material is available free of charge via the Internet at <http://pubs.acs.org>.

■ AUTHOR INFORMATION

Corresponding Author

*Tel: (+86) 21-5492-5085. Fax: (+86) 21-5492-5087. E-mail: zhengchao@sioc.ac.cn, slyou@sioc.ac.cn.

Notes

The authors declare no competing financial interest.

■ ACKNOWLEDGMENTS

The National Basic Research Program of China (973 Program 2010CB833300) and the National Natural Science Foundation (20923005, 21025209, 21121062) of China are acknowledged for generous financial support. We are also grateful to Prof. Yu-Xue Li at SIOC for helpful discussions.

■ REFERENCES

(1) Seminal reports: (a) Pictet, A.; Spengler, T. *Chem. Ber.* **1911**, *44*, 2030. (b) Tatsui, G. *J. Pharm. Soc. Jpn.* **1928**, *48*, 92. Reviews: (c) Cox, E. D.; Cook, J. M. *Chem. Rev.* **1995**, *95*, 1797. (d) Royer, J.; Bonin, M.; Micouin, L. *Chem. Rev.* **2004**, *104*, 2311. (e) Lorenz, M.; Linn, M. L. V.; Cook, J. M. *Curr. Org. Synth.* **2010**, *7*, 189. (f) Stöckigt, J.; Antonchick, A. P.; Wu, F.; Waldmann, H. *Angew. Chem., Int. Ed.* **2011**, *50*, 8538. (g) Kundu, B.; Agarwal, P. K.; Sharma, S. K.; Sawant, D.; Mandadapu, A. K.; Saifuddin, M.; Gupta, S. *Curr. Org. Synth.* **2012**, *9*, 357. Book chapter: (h) Menendez, P.; D'Acquarica, I.; Monache, G. D.; Ghirga, F.; Calcaterra, A.; Barba, M.; Macone, A.; Boffi, A.; Bonamore, A.; Botta, B. Production of Bioactives Compounds: The Importance of Pictet–Spengler Reaction in the XXI Century. In *Plant Bioactives and Drug Discovery: Principles, Practice, and Perspectives*; Cechinel-Filho, V., Ed.; Wiley: New York, 2012; pp 453–487. Selected recent examples of the asymmetric Pictet–Spengler reaction: (i) Yamada, H.; Kawate, T.; Matsumizu, M.; Nishida, A.; Yamaguchi, K.; Nakagawa, M. *J. Org. Chem.* **1998**, *63*, 6348. (j) Taylor, M. S.; Jacobsen, E. N. *J. Am. Chem. Soc.* **2004**, *126*, 10558. (k) Seayad, J.; Seayad, A. M.; List, B. *J. Am. Chem. Soc.* **2006**, *128*, 1086. (l) Raheem, I. T.; Thiara, P. S.; Peterson, E. A.; Jacobsen, E. N. *J. Am. Chem. Soc.* **2007**, *129*, 13404. (m) Wanner, M. J.; van der Haas, R. N. S.; de Cuba, K. R.; van Maarseveen, J. H.; Hiemstra, H. *Angew. Chem., Int. Ed.* **2007**, *16*, 7485. (n) Raheem, I. T.; Thiara, P. S.; Jacobsen, E. N. *Org. Lett.* **2008**, *10*, 1577. (o) Sewgobind, N. V.; Wanner, M. J.; Ingemann, S.; de Gelder, R.; van Maarseveen, J. H.; Hiemstra, H. *J. Org. Chem.* **2008**, *73*, 6405. (p) Muratore, M. E.; Holloway, C. A.; Pilling, A. W.; Storer, R. I.; Trevitt, G.; Dixon, D. J. *J. Am. Chem. Soc.* **2009**, *131*, 10796. (q) Klausen, R. S.; Jacobsen, E. N. *Org. Lett.* **2009**, *11*, 887. (r) Wanner, M. J.; Boots, R. N. A.; Eradus, B.; de Gelder, R.; van Maarseveen, J. H.; Hiemstra, H. *Org. Lett.* **2009**, *11*, 2579. (s) Holloway, C. A.; Muratore, M. E.; Storer, R. I.; Dixon, D. J. *Org. Lett.* **2010**, *12*, 4720. (t) Yin, W.; Kabir, S.; Wang, Z.; Rallapalli, S. K.; Ma, J.; Cook, J. M. *J. Org. Chem.* **2010**, *75*, 3339. (u) Wu, X.; Dai, X.; Fang, H.; Nie, L.; Chen, J.; Cao, W.; Zhao, G. *Chem.–Eur. J.* **2011**, *17*, 10510. (v) He, Y.; Lin, M.; Li, Z.; Liang, X.; Li, G.; Antilla, J. C. *Org. Lett.* **2011**, *13*, 4490. (w) Lee, Y.; Klausen, R. S.; Jacobsen, E. N. *Org. Lett.* **2011**, *13*, 5564. (x) Cheng, D.-J.; Wu, H.-B.; Tian, S.-K. *Org. Lett.* **2011**, *13*, 5636. (y) Herlé, B.; Wanner, M. J.; van Maarseveen, J. H.; Hiemstra, H. *J. Org. Chem.* **2011**, *76*, 8907. (z) Duce, S.; Pescioli, F.; Gramigna, L.; Bernardi, L.; Mazzanti, A.; Ricci, A.; Bartoli, G.; Bencivenni, G. *Adv. Synth. Catal.* **2011**, *353*, 860. (aa) Rueping, M.; Volla, C. M. R.; Bolte, M.; Rabbe, G. *Adv. Synth. Catal.* **2011**, *353*,

2853. (ab) Edwankar, C. R.; Edwankar, R. V.; Deschamps, J. R.; Cook, J. M. *Angew. Chem., Int. Ed.* **2012**, *51*, 11762. (ac) Huang, D.; Xu, F.; Lin, X.; Wang, Y. *Chem.–Eur. J.* **2012**, *18*, 3148. (ad) Cai, Q.; Liang, X.-W.; Wang, S.-G.; You, S.-L. *Org. Biomol. Chem.* **2013**, *11*, 1602.

(2) For recent reviews: (a) Edwankar, C. R.; Edwankar, R. V.; Namjoshi, O. A.; Rallapalli, S. K.; Yang, J.; Cook, J. M. *Curr. Opin. Drug Discovery Dev.* **2009**, *12*, 752. (b) Pulka, K. *Curr. Opin. Drug Discovery Dev.* **2010**, *13*, 669.

(3) (a) Williams, J. R.; Unger, L. R. *Chem. Commun.* **1970**, 1605. (b) Ungemach, F.; Cook, J. M. *Heterocycles* **1978**, *9*, 1089. (c) Bailey, P. D. *J. Chem. Res., Synop.* **1987**, 202. (d) Kawate, T.; Nakagawa, M.; Ogata, K.; Hino, T. *Heterocycles* **1992**, *33*, 801. (e) Edwankar, R. V.; Edwankar, C. R.; Namjoshi, O. A.; Deschamps, J. R.; Cook, J. M. *J. Nat. Prod.* **2012**, *75*, 181.

(4) (a) Jackson, A. H.; Smith, A. E. *Tetrahedron* **1965**, *21*, 989. (b) Jackson, A. H.; Smith, A. E. *Tetrahedron* **1968**, *24*, 403. (c) Jackson, A. H.; Smith, P. *Tetrahedron* **1968**, *24*, 2227. (d) Jackson, A. H.; Naidoo, B.; Smith, P. *Tetrahedron* **1968**, *24*, 6119. (e) Ibaceta-Lizana, J. S. L.; Jackson, A. H.; Prasitpan, N.; R. Shannon, P. V. *J. Chem. Soc., Perkin Trans. 2* **1987**, 1221.

(5) It was also found that direct attack at the C2 position could occur under certain circumstances and the selectivity was affected by many reaction parameters. Casnati, G.; Dossena, A.; Pochini, A. *Tetrahedron Lett.* **1972**, *52*, 5277.

(6) For theoretical studies that supported direct attack mechanism using the MNDO approach, see: (a) Kowalski, P.; Bojarski, A. J.; Mokrosz, J. L. *Tetrahedron* **1995**, *51*, 2737. (b) Kowalski, P.; Mokrosz, J. L. *Bull. Soc. Chim. Belg.* **1997**, *106*, 147.

(7) Maresh, J. J.; Giddings, L.-A.; Friedrich, A.; Loris, E. A.; Panjikar, S.; Trout, B. L.; Stöckigt, J.; Peters, B.; O'Connor, S. E. *J. Am. Chem. Soc.* **2008**, *130*, 710.

(8) Wu, Q.-F.; Zheng, C.; You, S.-L. *Angew. Chem., Int. Ed.* **2012**, *51*, 1680.

(9) (a) Wu, Q.-F.; He, H.; Liu, W.-B.; You, S.-L. *J. Am. Chem. Soc.* **2010**, *132*, 11418. (b) Wu, Q.-F.; Liu, W.-B.; Zhuo, C.-X.; Rong, Z.-Q.; Ye, K.-Y.; You, S.-L. *Angew. Chem., Int. Ed.* **2011**, *50*, 4455. (c) Zhuo, C.-X.; Liu, W.-B.; Wu, Q.-F.; You, S.-L. *Chem. Sci.* **2012**, *3*, 205.

(10) (a) Smith, M. B.; March, J. *March's Advanced Organic Chemistry* 5th ed.; Wiley-Interscience: New York, 2001; pp 1380–1384. For a related computational study, see: (b) Nakamura, K.; Osamura, Y. *J. Am. Chem. Soc.* **1993**, *115*, 9112.

(11) Selected examples for retention of migratory group configuration in the pinacol and Wagner–Meerwein-type rearrangement, see: (a) Beggs, J. J.; Meyers, M. B. *J. Chem. Soc. B* **1970**, 930. (b) Kirmse, W.; Gruber, W.; Knist, J. *Chem. Ber.* **1973**, *106*, 1376. (c) Shono, T.; Fujita, K.; Kumai, S. *Tetrahedron Lett.* **1973**, *14*, 3123. (d) Borodkin, G. I.; Panova, Y. B.; Shakirov, M. M.; Shubin, V. G. *J. Org. Chem. USSR* **1983**, *19*, 103.

(12) The TsOH-catalyzed allyl migration of the (3*S*,8*S*)-isomer of spiroindolenine **2a-epi** was also considered. The reaction profile and the structural features of the key transition states are similar to that of the (3*S*,8*R*)-isomer **2a** presented in the text. See the Supporting Information for details.

(13) For a very recent report of the intramolecular rearrangement of the 3,3-disubstituted indolenines to the corresponding 2,3-disubstituted indoles, see: Nguyen, Q.; Nguyen, T.; Driver, T. G. *J. Am. Chem. Soc.* **2013**, *135*, 620.

(14) The NBO charges on the allyl and methylene group in **5a** are +0.063 and +0.142, respectively.

(15) The Gibbs free energy of the phenyl-substituted spiroindolenine **2c** is higher than the corresponding benzyl migration product **4c** by 24.2 kcal/mol.

(16) The Gibbs free energy of the N-Bn and N-Tf aza-spiroindolenines **2d** and **2e** are higher than the corresponding tetrahydro- β -carboline compounds **4d** and **4e** by 16.2 and 20.3 kcal/mol, respectively.

(17) The NBO charges on the N-Bn moiety in **8d** and **8d'** are –0.005 and –0.022, respectively.

(18) The reaction profile of the rearrangement of the N-Bn aza-spiroindolenine is similar to that of the N-H analogue calculated by Stöckigt, Peters, and O'Connor et al. See ref 7.

(19) The value of the stabilization energy must be overestimated because the electron occupancy of both the donor and acceptor orbital in this structure are somewhat deviated from the ideal "full" and "empty" circumstances. See the Supporting Information for details.

(20) The NBO charge on the N-Tf moiety in **8e** and **8e'** are -0.379 and -0.201 , respectively.

(21) Genesan, A.; Hoothcock, C. H. *Tetrahedron Lett.* **1993**, *34*, 439.

(22) During the preparation of this manuscript, Bandini and Miscione et al. reported a mechanistic research of a related enantioselective gold-catalyzed allylation of indoles and alcohols. In that study, the enantioenriched tetrahydrocarbazole products are suggested to be formed via a stepwise S_N2' process. The authors demonstrated that the formation of a spiroindolenine intermediate and subsequent migration is not a competitive pathway. Bandini, M.; Bottoni, A.; Chiarucci, M.; Cera, G.; Miscione, G. P. *J. Am. Chem. Soc.* **2012**, *134*, 20690.

(23) Frisch, M. J. et al. Gaussian09, Revision A.01; Gaussian, Inc., Wallingford, CT, 2009.

(24) (a) Perdew, J. P.; Burke, K.; Ernzerhof, M. *Phys. Rev. Lett.* **1996**, *77*, 3865. (b) Perdew, J. P.; Burke, K.; Ernzerhof, M. *Phys. Rev. Lett.* **1997**, *78*, 1396.

(25) Marenich, A. V.; Cramer, C. J.; Truhlar, D. G. *J. Phys. Chem. B* **2009**, *113*, 6378.

(26) (a) Zhao, Y.; Truhlar, D. G. *Theor. Chem. Acc.* **2008**, *120*, 215.

(b) Zhao, Y.; Truhlar, D. G. *Acc. Chem. Res.* **2008**, *41*, 157.

(27) Single-point calculations of the transition states and intermediates of the reaction profile of **5a** and **5e** (structures shown in Figures 1 and 6) were performed at the M06-2X/6-311+G(d,p) level of theory in THF (SMD model). The energetic trends are the same as that obtained with PBE1PBE functional. The small energetic deviation does not alter the conclusion drawn in this paper. See the Supporting Information for details.

(28) Legault, C. Y. CYLView, 1.0b; Université de Sherbrooke, Montreal, Québec, Canada, 2009; <http://www.cylview.org>.